Article

A New Empirical Model for Radar Scattering from Bare Soil Surfaces

Nicolas Baghdadi [1,*], Mohammad Choker [1], Mehrez Zribi [2], Mohammad El Hajj [1], Simonetta Paloscia [3], Niko E. C. Verhoest [4], Hans Lievens [4,5], Frederic Baup [2] and Francesco Mattia [6]

[1] IRSTEA, UMR TETIS, 500 rue François Breton, F-34093 Montpellier CEDEX 5, France; mohammad.choker@teledetection.fr (M.C.); mohammad.el-hajj@teledetection.fr (M.E.H.)
[2] CESBIO, 18 av. Edouard Belin, bpi 2801, 31401 Toulouse CEDEX 9, France; mehrez.zribi@ird.fr (M.Z.); frederic.baup@cesbio.cnes.fr (F.B.)
[3] CNR-IFAC, via Madonna del Piano, 10, 50019 Florence, Italy; s.paloscia@ifac.cnr.it
[4] Laboratory of Hydrology and Water Management, Ghent University, B-9000 Ghent, Belgium; niko.verhoest@UGent.be (N.E.C.V.); hans.lievens@UGent.be (H.L.)
[5] Global Modeling and Assimilation Office, NASA Goddard Space Flight Center, Greenbelt, MD 20771, USA
[6] CNR-ISSIA, via Amendola 122/D, 70126 Bari, Italy; mattia@ba.issia.cnr.it
* Correspondence: nicolas.baghdadi@teledetection.fr; Tel.: +33-4-6754-8724

Abstract: The objective of this paper is to propose a new semi-empirical radar backscattering model for bare soil surfaces based on the Dubois model. A wide dataset of backscattering coefficients extracted from synthetic aperture radar (SAR) images and in situ soil surface parameter measurements (moisture content and roughness) is used. The retrieval of soil parameters from SAR images remains challenging because the available backscattering models have limited performances. Existing models, physical, semi-empirical, or empirical, do not allow for a reliable estimate of soil surface geophysical parameters for all surface conditions. The proposed model, developed in HH, HV, and VV polarizations, uses a formulation of radar signals based on physical principles that are validated in numerous studies. Never before has a backscattering model been built and validated on such an important dataset as the one proposed in this study. It contains a wide range of incidence angles (18°–57°) and radar wavelengths (L, C, X), well distributed, geographically, for regions with different climate conditions (humid, semi-arid, and arid sites), and involving many SAR sensors. The results show that the new model shows a very good performance for different radar wavelengths (L, C, X), incidence angles, and polarizations (RMSE of about 2 dB). This model is easy to invert and could provide a way to improve the retrieval of soil parameters.

Keywords: new backscattering model; Dubois model; SAR images; soil parameters

1. Introduction

Soil moisture content and surface roughness play important roles in meteorology, hydrology, agronomy, agriculture, and risk assessment. These soil surface characteristics can be estimated using synthetic aperture radar (SAR). Today, several high-resolution SAR images can be acquired on a given study site with the availability of SAR data in the L-band (ALOS-2), the C-band (Sentinel-1), and the X-band (TerraSAR-X, COSMO-SkyMed). In addition, it is possible to obtain SAR and optical data for global areas at high spatial and temporal resolutions with free and open access Sentinel-1/2 satellites (six days with the two Sentinel-1 satellites and five days with the two Sentinel-2 satellites at 10 m spatial resolution). This availability of both Sentinel-1 satellites and Sentinel-2 sensors, in addition to

Landsat-8 (also free and open access), allows the combination of SAR and optical data to estimate soil moisture and vegetation parameters in operational mode.

The retrieval of soil moisture content and surface roughness requires the use of radar backscatter models capable of correctly modelling the radar signal for a wide range of soil parameter values. This estimation from imaging radar data implies the use of backscattering electromagnetic models, which can be physical, semi-empirical, or empirical. The physical models (e.g., integral equation model "IEM", small perturbation model "SPM", geometrical optic model "GOM", physical optic model "POM", etc.), based on physical approximations corresponding to a range of surface conditions (moisture and roughness), provide site-independent relationships, but have limited validity depending upon the soil roughness. As for semi-empirical or empirical models, they are often difficult to apply to sites other than those on which they were developed and are generally valid only for specific soil conditions. The empirical models are often favored by users because the models are easier to implement and invert [1–7].

Among the numerous semi-empirical models reported in the literature, the most popular are those developed over bare soils by Oh et al. [8–11] and Dubois et al. [12]. The Oh model uses the ratios of the measured backscatter coefficients HH/VV and HV/VV to estimate volumetric soil moisture (*mv*) and surface roughness (*Hrms*), while the Dubois model links the backscatter coefficients in HH and VV polarizations to the soil's dielectric constant and surface roughness. Extensive studies evaluated various semi-empirical models, but mixed results have been obtained. Some studies show good agreement between measured backscatter coefficients and those predicted by the models, while others have found great discrepancies between them (e.g., [13–16]). The discrepancy between simulations and measurements often reach several decibels, making soil parameter estimates unusable.

The objective of this paper is to propose a robust, empirical, radar backscattering model based on the Dubois model. First, the performance of the Dubois model is analyzed using a large dataset acquired at several worldwide study sites by numerous SAR sensors. The dataset consists of SAR data (multi-angular and multi-frequency) and measurements of soil moisture and surface roughness over bare soils. Then, the different terms of Dubois equations that describe the dependence between the SAR signal and both sensor and soil parameters have been validated or modified to improve the modelling of the radar signal. Ultimately, a new semi-empirical backscattering model has been developed for radar scattering in the HH, VV, and HV polarization from bare soil surfaces.

After a description of the dataset in Section 2, Section 3 describes and analyzes the potential and the limitations of the Dubois model in radar signal simulations over bare soils. In Section 4, the new model is described and its performance is evaluated for different available SAR data (L-, C- and X-bands, incidence angles between 20° and 45°). Conclusions are presented in Section 5.

2. Dataset Description

A wide experimental dataset was used, consisting of SAR images and ground measurements of soil moisture content and roughness collected over bare soils at several agricultural study sites (Table 1). SAR images were acquired by various airborne and spaceborne sensors (AIRSAR, SIR-C, JERS-1, PALSAR-1, ESAR, ERS, RADARSAT, ASAR, and TerraSAR-X). The radar data were available in L-, C-, and X-bands (approximately 1.25 GHz, 5.3 GHz, and 9.6 GHz, respectively); with incidence angles between 18° and 57°; and in HH, VV, and HV polarizations. For several reference plots, the mean backscatter coefficients have been obtained from radiometrically and geometrically calibrated SAR images by averaging backscatter coefficient values for each plot for all pixels within the plot.

In addition, in situ measurements of soil moisture (*mv*) were available for each reference plot. The soil water content was collected from the top 5–10 cm of each reference plot at several locations using the gravimetric method and a calibrated time domain reflectometry (TDR) probe. In practice, the soil moisture for each reference plot was assumed to be equal to the mean of all measurements carried out on the reference plot within a few hours of the SAR overpasses. In our experimental dataset, the soil moisture ranged from 2–47 vol%.

Table 1. Description of the dataset used in this study. "Fr": France, "It": Italy, "Ge": Germany, "Be": Belgium, "Lu": Luxembourg, "Ca": Canada, "Tu": Tunisia.

Site	SAR Sensor	Freq	Year	Number of Data Measurements
Orgeval (Fr) [17] Orgeval (Fr) [17–19] Orgeval (Fr) [19] Orgeval (Fr) [20]	SIR-C SIR-C, ERS, ASAR PALSAR-1 TerraSAR-X	L C L X	1994 1994; 1995; 2008; 2009; 2010 2009 2008, 2009, 2010	
Pays de Caux (Fr) [21,22]	ERS; RADARSAT	C	1998; 1999	
Villamblain (Fr) [23–25] Villamblain (Fr) [13,19]	ASAR TerraSAR-X	C X	2003; 2004; 2006 2008; 2009	
Thau (Fr) [26]	RADARSAT TerraSAR-X	C X	2010; 2011 2010	
Touch (Fr) [23,27]	ERS-2; ASAR	C	2004; 2006; 2007	
Mauzac (Fr) [13]	TerraSAR-X	X	2009	
Garons (Fr) [13]	TerraSAR-X	X	2009	➤ HH: 1569 measurements
Kairouan (Tu) [28] Kairouan (Tu) [13,28,29]	ASAR TerraSAR-X	C X	2012 2010; 2012; 2013; 2014	- 144 in L-band - 997 in C-band - 428 in X-band
Yzerons (Fr) [30]	TerraSAR-X	X	2009	➤ VV: 930 measurements
Versailles (Fr) [13]	TerraSAR-X	X	2010	- 71 in L-band
Seysses (Fr) [13]	TerraSAR-X	X	2010	- 640 in C-band - 219 in X-band
Chateauguay (Ca) [21]	RADARSAT	C	1999	
Brochet (Ca) [21]	RADARSAT	C	1999	➤ HV: 605 measurements
Alpilles (Fr) [21]	ERS; RADARSAT	C	1996; 1997	- 7 in L-band
Sardaigne (It) [31]	ASAR; RADARSAT	C	2008; 2009	- 538 in C-band - 60 in X-band
Saint Lys (Fr) [32]	PALSAR-1	L	2010	
Matera (It) [33]	SIR-C	L	1994	
Alzette (Lu) [34]	PALSAR-1	L	2008	
Dijle (Be) [34]	PALSAR-1	L	2008; 2009	
Zwalm (Be) [34]	PALSAR-1	L	2007	
Demmin (Ge) [34]	ESAR	L	2006	
Montespertoli (It) [35] Montespertoli (It) [36] Montespertoli (It) [37]	AIRSAR SIR-C JERS-1	L L; C L	1991 1994 1994	

The roughness was defined by the standard deviation of surface height (*Hrms*) available for each reference plot. From roughness profiles sampled for each reference plot using mainly laser or needle profilometers (mainly 1 m and 2 m long and with 1 cm and 2 cm sampling intervals), the mean of all experimental autocorrelation functions was calculated to estimate the *Hrms* measurement. However, for some in situ measurement campaigns, the meshboard technique was used for estimating the roughness parameters. In our dataset, *Hrms* surface height ranged from 0.2–9.6 cm (*k Hrms* ranged from 0.2–13.4, *k* was the radar wave number).

A total of 1569 experimental data acquisitions with radar signal, soil moisture content, and roughness were available for HH polarization, 930 for VV polarization, and 605 for HV polarization.

3. Validation and Analysis of the Dubois Model

3.1. Description of the Dubois Model

Dubois et al. [12] proposed an empirical model to model radar backscatter coefficients in HH and VV polarizations (σ^0_{HH} and σ^0_{VV}) for bare soil surfaces. The expressions of σ^0_{HH} and σ^0_{VV} depend on the radar wave incidence angle (θ, in radians), the real part of the soil dielectric constant (ε), the rms surface height of the soil (*Hrms*), and the radar wavelength ($\lambda = 2\pi/k$, where *k* is the radar wavenumber):

$$\sigma^0_{HH} = 10^{-2.75} \left(\frac{\cos^{1.5}\theta}{\sin^5\theta} \right) 10^{0.028\varepsilon\tan\theta} \, (k\,Hrms\sin\theta)^{1.4} \, \lambda^{0.7} \tag{1}$$

$$\sigma_{VV}^0 = 10^{-2.35} \left(\frac{\cos^3\theta}{\sin^3\theta} \right) 10^{0.046\varepsilon\tan\theta} \, (k\,Hrms\sin\theta)^{1.1} \, \lambda^{0.7} \tag{2}$$

σ_{HH}^0 and σ_{VV}^0 are given in a linear scale. λ is in cm. The validity of the Dubois model is defined as follows: $k\,Hrms \leq 2.5$, $mv \leq 35$ vol%, and $\theta \geq 30°$.

3.2. Comparison between Simulated and Real Data

The Dubois model shows an overestimation of the radar signal by 0.7 dB in HH polarization and an underestimation of the radar signal by 0.9 dB in VV polarization for all data combined (Table 2). The results show that the overestimation in HH is of the same order for L-, C-, and X-bands (between 0.6–0.8 dB). For the L-band, a slight overestimation of approximately 0.2 dB of SAR data is observed in VV polarization. Additionally, in VV polarization, the Dubois model-based simulations underestimate the SAR data in the C- and X-bands by approximately 0.7 dB and 2.0 dB, respectively.

The rms error (RMSE) is approximately 3.8 dB and 2.8 dB in HH and VV, respectively (Table 2). Analysis of the RMSE according the radar frequency band (L-, C-, and X-, separately) shows in HH an increase of the RMSE with the radar frequency (2.9 dB in the L-band, 3.7 dB in the C-band, and 4.1 dB in the X-band). In VV polarization, the quality of Dubois simulations (RMSE) is similar for the L- and C-bands, but is less accurate in the X-band (2.3 dB in the L-band, 2.6 dB in the C-band, and 3.2 dB in the X-band).

Table 2. Comparison between the Dubois model and real data for all data and by range of *kHrms*, soil moisture (*mv*), and incidence angle (θ). Bias = real data − model.

	Dubois for HH		Dubois for VV	
	Bias (dB)	**RMSE (dB)**	**Bias (dB)**	**RMSE (dB)**
For all data	−0.7	3.8	+0.9	2.8
L-band	−0.8	2.9	−0.2	2.3
C-band	−0.6	3.7	+0.7	2.6
X-band	−0.7	4.1	+2.0	3.2
kHrms < 2.5	+0.4	3.4	+1.3	2.9
kHrms > 2.5	−2.7	4.5	−0.1	2.5
mv < 20 vol%	−2.0	4.3	+0.9	2.8
mv > 20 vol%	+0.5	3.2	+0.9	2.8
θ < 30°	−4.1	5.4	−0.6	2.9
θ > 30°	+0.6	3.0	+1.5	2.7

In addition, the agreement between the Dubois model simulations and SAR data is analyzed according to soil roughness, moisture content, and incidence angle (Figures 1 and 2). The results indicate a slight underestimation of the radar signal by the Dubois model in the case of *kHrms* lower than 2.5 (Dubois validation domain) for both HH and VV polarizations (Figures 1b and 2b; Table 2). For surfaces with a roughness *kHrms* greater than 2.5, an overestimation of the radar signal is obtained with the Dubois model in HH, while the model works correctly in VV (Figures 1b and 2b; Table 2). Higher under- and overestimations are observed in HH than they are in VV (reaching approximately 10 dB in HH).

Analysis of the error as a function of soil moisture (*mv*) shows that for both VV-polarized data, whatever the *mv* values, and HH-polarized data with *mv* values higher than 20 vol%, the observed bias between real and simulated data is small (Figures 1c and 2c; Table 2). However, a strong overestimation of the radar signal is observed by the Dubois model in HH for *mv* values lower than 20 vol% (−2.0 dB, Table 2).

Finally, the discrepancy between SAR and the model is larger in HH for incidence angles lower than 30° (outside of the Dubois validity domain) than for incidence angles higher than 30° (Table 2). The Dubois model strongly overestimates the radar signal in HH for incidence angles lower than 30°

but agrees closely with the measured data for incidence angles higher than 30° (Figures 1d and 2d; Table 2). In VV polarization, the Dubois model slightly overestimates the radar signal for incidence angles lower than 30° and underestimates the signal for incidence angles higher than 30° by +1.5 dB (Figures 1d and 2d; Table 2).

In conclusion, the Dubois model simulates VV better than it does HH (RMSE = 2.8 and 3.8 dB, respectively). The disagreements observed between the Dubois model and measured data are not limited to data that are outside the optimal application domain of the Dubois model.
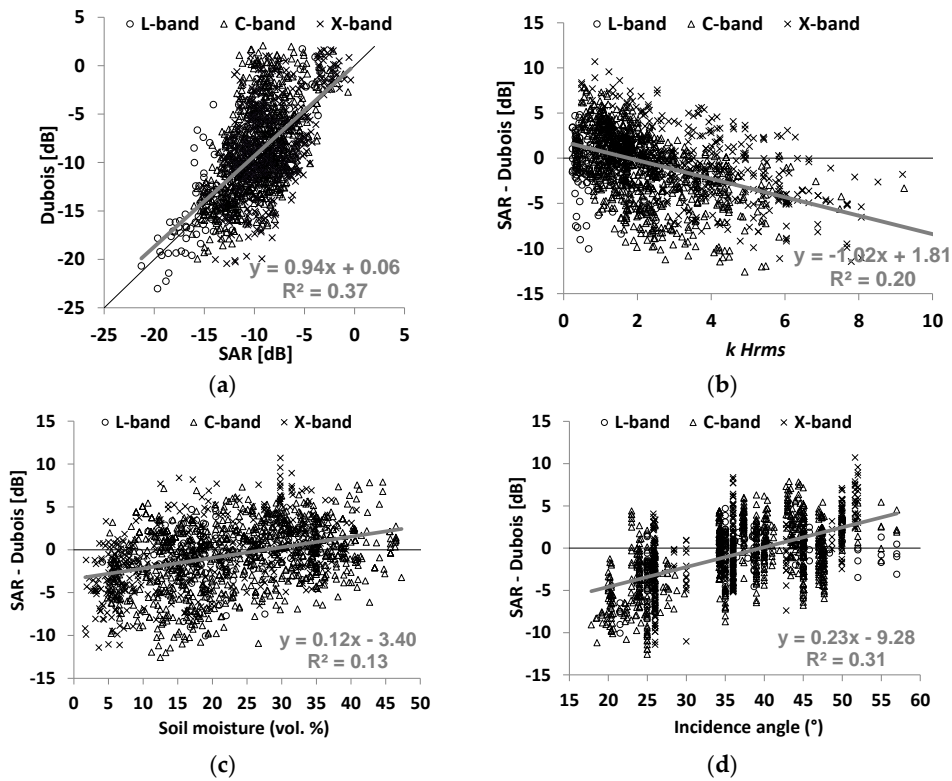
Figure 1. For HH polarization, (**a**) comparison between radar backscattering coefficients calculated from SAR images and estimated from the Dubois model; (**b**) the difference between the SAR signal and the Dubois model relative to soil roughness (*kHrms*); (**c**) the difference between the SAR signal and the Dubois model relative to soil moisture (*mv*); and (**d**) the difference between the SAR signal and the Dubois model relative to incidence angle. The best regression model is plotted in gray.
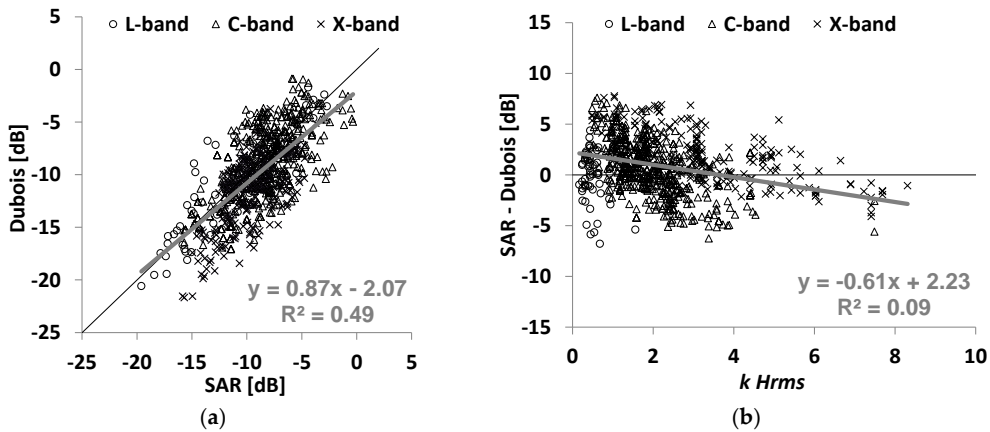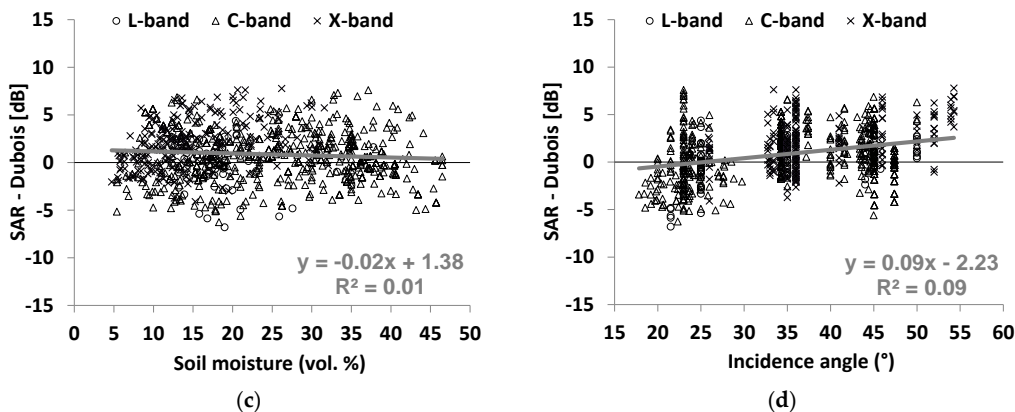

Figure 2. *Cont.*

Figure 2. For VV polarization, (**a**) comparison between radar backscattering coefficients calculated from SAR images and estimated from the Dubois model; (**b**) the difference between the SAR signal and the Dubois model relative to soil roughness (*kHrms*); (**c**) the difference between the SAR signal and the Dubois model relative to soil moisture (*mv*); and (**d**) the difference between the SAR signal and the Dubois model relative to incidence angle. The best regression model is plotted in gray.

4. New Empirical Model

4.1. Methodology

The disagreement observed between the measured and modelled radar signal encouraged us to develop a new empirical backscattering model using SAR observations and soil in situ measurements. The new model is based on the Dubois model and uses the dependency observed between the SAR signal and soil parameters according to results obtained in various studies. For bare soils, the backscattering coefficient depends on soil parameters (roughness and moisture) and SAR instrumental parameters (incidence angle, polarization, and wavelength). For bare soils, the radar signal in *pq* polarization (*p* and *q* = H or V, with HV = VH) can be expressed as the product of three components:

$$\sigma^{\circ}_{pq} = f_{pq}\left(\theta\right) \ g_{pq}\left(mv, \theta\right) \ \Gamma_{pq}\left(kHrms, \theta\right) \tag{3}$$

The radar backscatter coefficient is related to the incidence angle (θ) by the relation $f_{pq}\left(\theta\right) = \alpha(cos\theta)^{\beta}$ [38–40]. This relationship describes the decrease of σ° with the incidence angle (the decrease is higher for low angles than for high angles).

The second term represents the relationship between the radar backscatter coefficient and soil moisture (*mv*). The results obtained in several investigations show that, for bare soils, the radar signal (σ°) in decibels increases linearly with soil moisture (*mv*) when *mv* is in the range between approximately 5–35 vol% (e.g., [5,6,19,41]). In the linear scale $g_{pq}\left(mv, \theta\right)$ can be written as $\delta \ 10^{\gamma \ mv}$. The sensitivity of the radar signal to the soil moisture γ depends on θ. Higher sensitivity is observed for lower than for higher incidence angles (e.g., [42,43]). To include this dependence on the incidence angle, the soil moisture value is multiplied with the term $cotan\left(\theta\right)$. Thus, $g_{pq}\left(mv, \theta\right)$ can be written as $\delta \ 10^{\gamma \ cotan(\theta) \ mv}$.

The last term $\Gamma_{pq}\left(kHrms, \theta\right)$ represents the behavior of σ° with soil roughness. An exponential or logarithmic function is often used to express the radar signal (in dB) in terms of surface roughness ([7,41,44,45]). For a logarithmic behavior of σ° (dB) with *k Hrms*, Γ_{pq} in the linear scale can be written as $\mu \left(kHrms\right)^{\xi}$. Baghdadi et al. [22] showed that at high incidence angles, the radar return is highly sensitive to surface roughness and shows much larger dynamics than at a low incidence angle. In addition, the term $sin\left(\theta\right)$ is intended to include this dependence with the incidence angle: $\Gamma_{pq} = \mu \left(kHrms\right)^{\xi \ sin(\theta)}$.

Finally, the relationship between the radar backscattering coefficient (σ°) and the soil parameters (soil moisture and surface roughness) for bare soil surfaces can be written as Equation (4):

$$\sigma^\circ_{pq} = \delta(cos\theta)^\beta \, 10^{\gamma \, cotan(\theta) \, mv} \, (kHrms)^{\xi \, sin(\theta)} \tag{4}$$

The coefficients δ, β, γ, and ξ are then estimated for each radar polarization using the method of least squares by minimizing the sum of squares of the differences between the measured and modelled radar signal. The error in the modelling of radar backscatter coefficients by the new backscattering model was assessed for each polarization using a five-fold cross-validation to validate the predictive performance of the new model. To conduct the five-fold cross-validation, the dataset was first randomly divided into five equal size subsets. Next, four of the subsets are used to train the new model and one was retained to validate its predictive performance. The cross-validation process was then repeated five times, with each of the five sub-datasets used exactly once as the validation data. The final validation result combines the five validation results. The advantage of this method over repeated random sub-sampling is that all observations are used for both training and validation, and each observation is used for validation exactly once.

The fitting of various coefficients parameter in the Equation (4) was done using the entire dataset (fitting errors are about 2 dB for all polarizations). This fitting allows writing σ° as a function of the rms surface height (*Hrms*) and incidence angle (*θ*), by Equations (5)–(7):

$$\sigma^\circ_{HH} = 10^{-1.287}(cos\,\theta)^{1.227} \, 10^{0.009 \, cotan(\theta) \, mv} \, (kHrms)^{0.86 \, sin(\theta)} \tag{5}$$

$$\sigma^\circ_{VV} = 10^{-1.138}(cos\,\theta)^{1.528} \, 10^{0.008 \, cotan(\theta) \, mv} \, (kHrms)^{0.71 \, sin(\theta)} \tag{6}$$

$$\sigma^\circ_{HV} = 10^{-2.325}(cos\,\theta)^{-0.01} \, 10^{0.011 \, cotan(\theta) \, mv} \, (kHrms)^{0.44 \, sin(\theta)} \tag{7}$$

where θ is expressed in radians and *mv* is in vol%. Equations (5)–(7) show that the sensitivity (γ) of the radar signal to the soil moisture in the decibel scale is 0.25 dB/vol% in HH polarization, 0.22 dB/vol% in VV polarization, and 0.30 dB/vol% in HV polarization for an incidence angle of 20°. This sensitivity decreases to 0.09 dB/vol% in HH, 0.08 dB/vol% in VV, and 0.11 dB/vol% for an incidence angle of 45°. As for the signal's sensitivity to soil roughness, it is of the same order of magnitude in HH and VV, and twice as large as the HV signal. The availability of a backscatter model for the cross-polarization component is required because most spaceborne SAR acquisitions are made with one co-polarization and one cross-polarization, in the case of a dual-polarization mode.

4.2. Results and Discussion

4.2.1. Performance of the New Model

Results show that the new model provides more accurate results. The biases and the RMSE decrease for both HH and VV polarizations. The RMSE decreases from 3.8 dB to 2.0 dB for HH and from 2.8 dB to 1.9 dB for VV (Table 3). In addition, the high over- or underestimations of radar backscattering coefficients observed with the Dubois model according to soil moisture, surface roughness, and radar incidence angle are clearly eliminated with the new model (Figures 3 and 4).

Analysis of the new model's performance for each radar wavelength, separately (L-, C- and X-bands), shows that the most significant improvement is observed in the X-band with an RMSE that decreases from 4.1 dB to 1.9 dB in HH and from 3.2 dB to 1.8 dB in VV. In the L-band, the performance of the new model is no better than that of the Dubois model because the RMSE decreases slightly with the new model, from 3.0 dB to 2.3 dB in HH, and remains similar in VV (RMSE = 2.3 dB with the Dubois model and 2.7 dB with the new model). The improvement is also important for the C-band with an RMSE that decreases from 3.7 dB to 1.9 dB in HH and from 2.6 dB to 1.9 dB in VV. With respect to bias, the results show that it decreases with the new model for all radar wavelengths. In addition,

the new model does not show bias according to the range of soil moisture, surface roughness, and radar incidence angle.
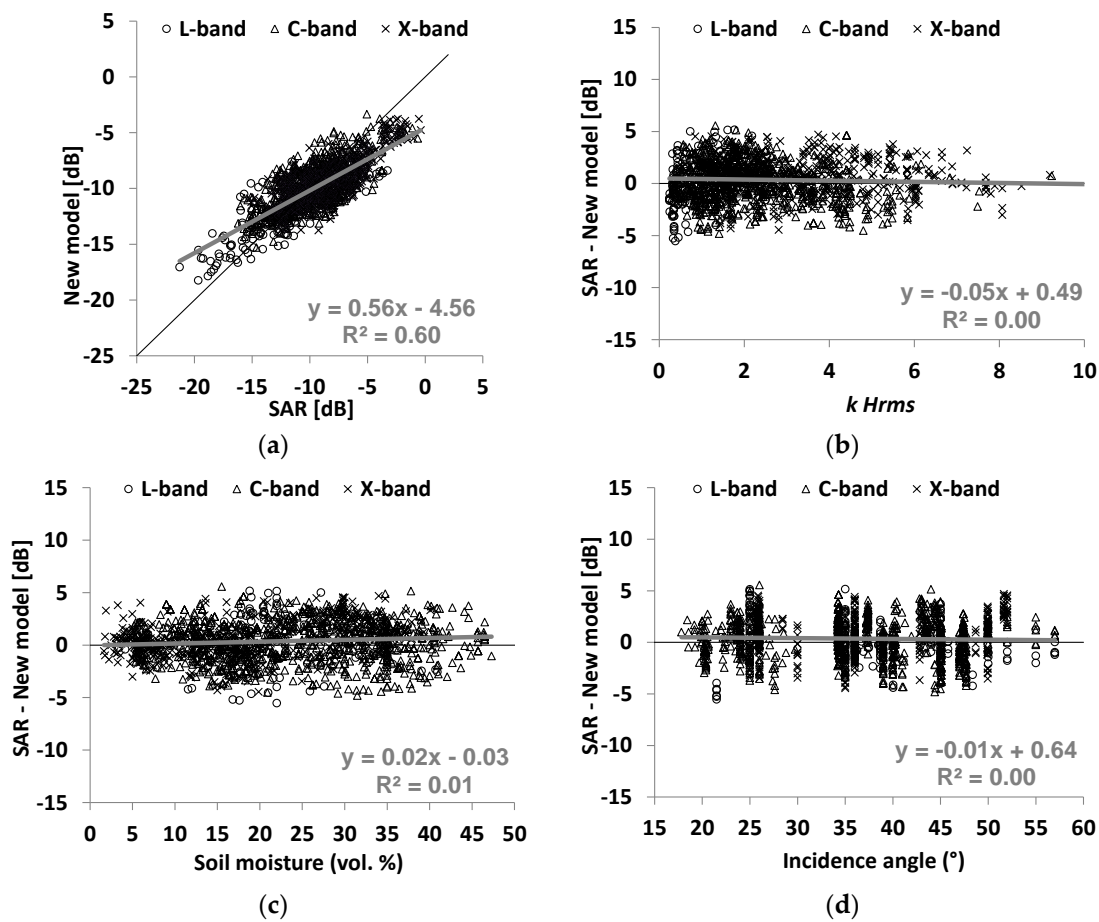

Figure 3. (**a**) Comparison between σ° modelled in the new model and σ° measured (for all SAR bands) for HH polarization; (**b**) the difference between SAR and the new model as a function of surface roughness (*kHrms*); (**c**) the difference between SAR and the new model as a function of soil moisture (*mv*), and (**d**) the difference between SAR and the new model as a function of incidence angle. The best regression model is plotted in gray.

Table 3. Comparison between the results obtained with the Dubois model and those obtained with the new model. Bias = real − model.

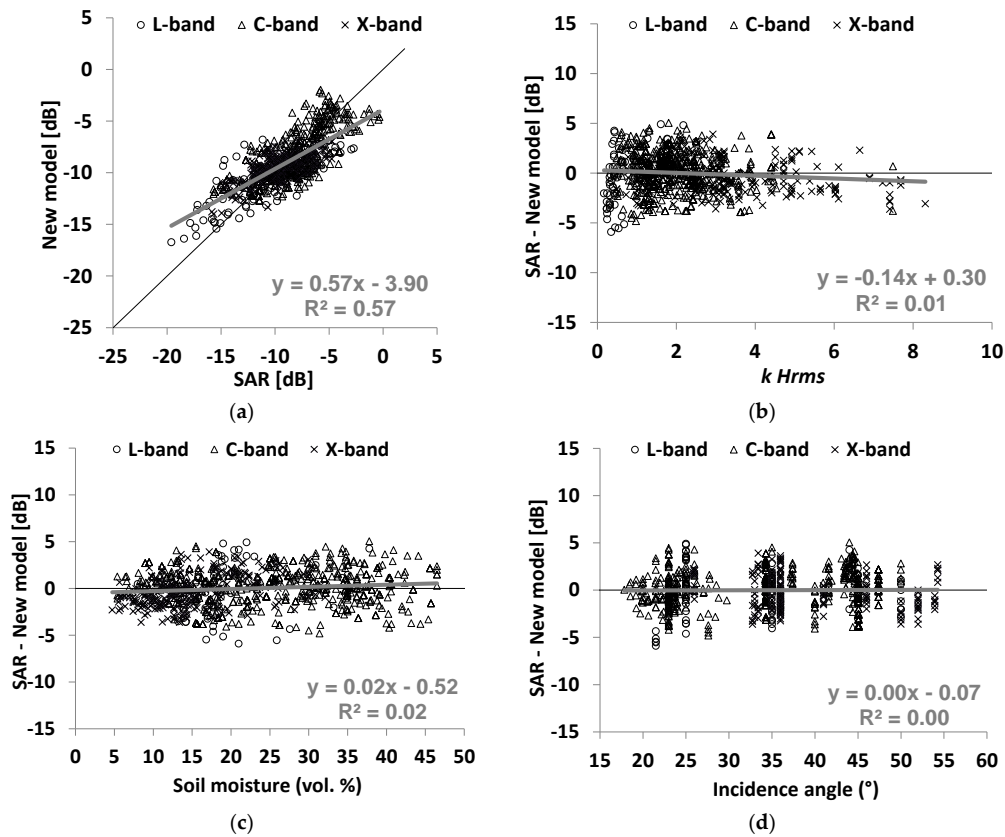|	Dubois for HH and VV		New Model	
	Bias (dB)	RMSE (dB)	Bias (dB)	RMSE (dB)
HH for all data	−0.7	3.8	0.4	2.0
VV for all data	+0.9	2.8	0.0	1.9
HV for all data	-	-	0.0	2.1
HH, L-band	−0.8	2.9	−0.1	2.3
HH, C-band	−0.6	3.7	+0.3	1.9
HH, X-band	−0.7	4.1	0.7	1.9
VV, L-band	−0.2	2.3	−0.1	2.7
VV, C-band	+0.7	2.6	+0.1	1.9
VV, X-band	+2.0	3.2	−0.4	1.8
HV, L-band	-	-	−1.3	1.6
HV, C-band	-	-	+0.2	2.2
HV, X-band	-	-	−1.3	1.9

Figure 4. (**a**) Comparison between $\sigma°$ in the new model and $\sigma°$ measured (for all SAR bands) for VV polarization; (**b**) the difference between SAR and the new model as a function of surface roughness (*kHrms*); (**c**) the difference between SAR and the new model as a function of soil moisture (*mv*); and (**d**) the difference between SAR and the new model as a function of incidence angle. The best regression model is plotted in gray.

The comparison between the new model simulations in HV polarization Equation (7) and the real data (SAR data) shows an RMSE of 2.1 dB (Table 3) (1.6 dB in the L-band, 2.2 dB in the C-band, and 1.9 dB in the X-band). The bias ($\sigma°$SAR—model) is −1.3 dB in the L-band, 0.2 dB in the C-band, and −1.3 dB in the X-band. Figure 5 shows also that the new model correctly simulates the radar backscatter coefficient in HV for all ranges of soil moisture, surface roughness, and radar incidence angle.
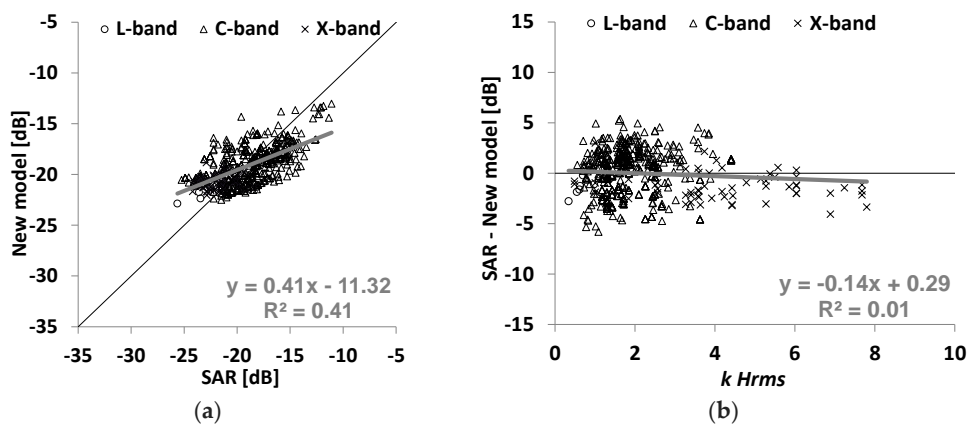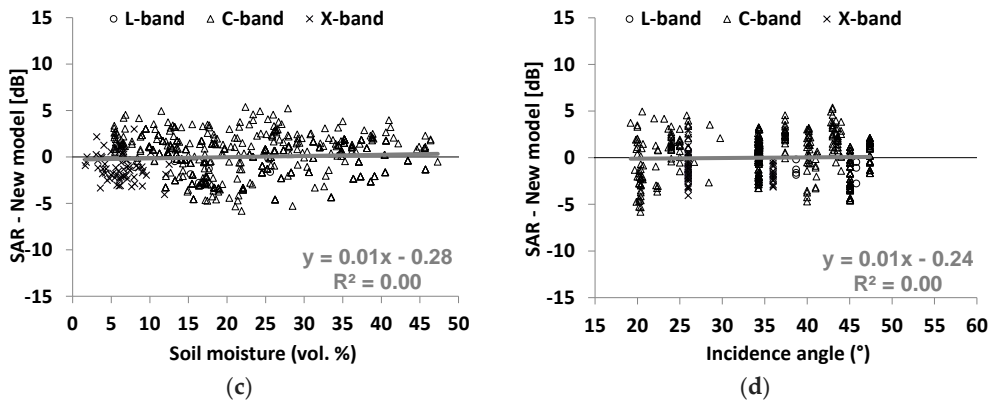

Figure 5. *Cont.*

(c)　　　　　　　　　　　　　　　　　　(d)

Figure 5. (**a**) Comparison between $\sigma°$ in the new model and $\sigma°$ measured (for all SAR bands) for HV polarization; (**b**) the difference between SAR and the new model as a function of *kHrms*; (**c**) the difference between SAR and the new model as a function of *mv*; and (**d**) the difference between SAR and the new model as a function of incidence angle. The best regression model is plotted in gray.

4.2.2. Behavior of the New Model

The physical behavior of the new radar backscatter model was studied as a function of the incidence angle (θ), soil moisture (*mv*), and surface roughness (*kHrms*).

Figure 6 shows that the radar signal is strongly sensitive to surface roughness, especially for small values of *kHrms*. In addition, this sensitivity increases with the incidence angle. Concerning the influence of polarization, the new model shows, as do many theories and experimental studies, that a given soil roughness leads to slightly higher signal dynamics with the soil moisture in HH than in VV polarization [17,46]. The radar signal $\sigma°$ increases with *kHrms*. This increase is higher for either low *kHrms* values or high θ values than it is for either high *kHrms* values or low θ values. For $\theta = 45°$, $\sigma°$ increases approximately 8 dB in HH and 6.5 dB in VV when *kHrms* increases from 0.1 to 2 compared with only 3 dB when *kHrms* increases from two to six (for both HH and VV). This dynamic of $\sigma°$ is only half for $\theta = 25°$ in comparison to that for $\theta = 45°$. In HV, the dynamic of $\sigma°$ to *kHrms* is half that observed for HH and VV.

The behavior of $\sigma°$ according to soil moisture shows a larger increase of $\sigma°$ with *mv* for low incidence angles than for high incidence angles. Figure 6 shows that $\sigma°_{HH}$ and $\sigma°_{VV}$ increase approximately 6 dB for $\theta = 25°$ compared with only 3 dB for $\theta = 45°$ when *mv* increases from five to 35 vol%. In HV, the signal increases approximately 7.5 dB for $\theta = 25°$ and 3.5 dB for $\theta = 45°$ when *mv* increases from 5 to 35 vol%.
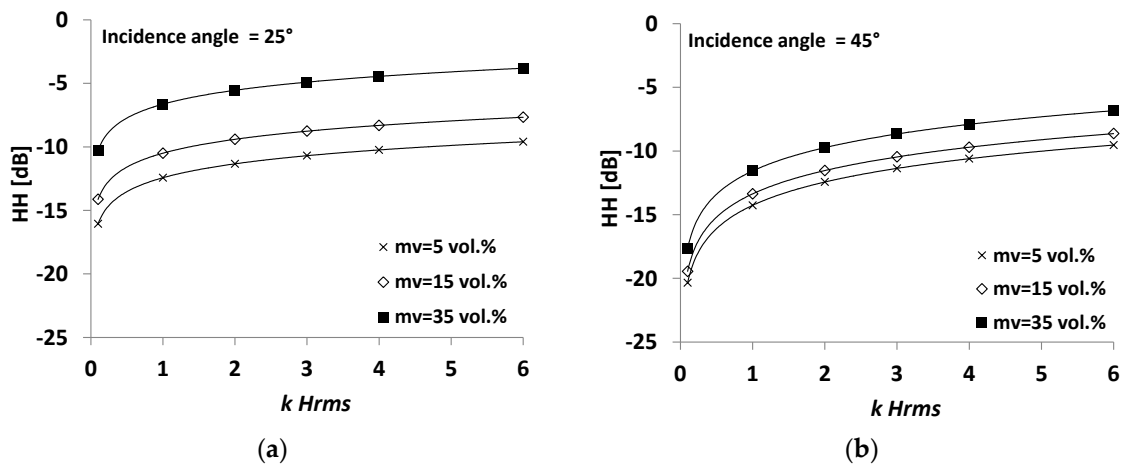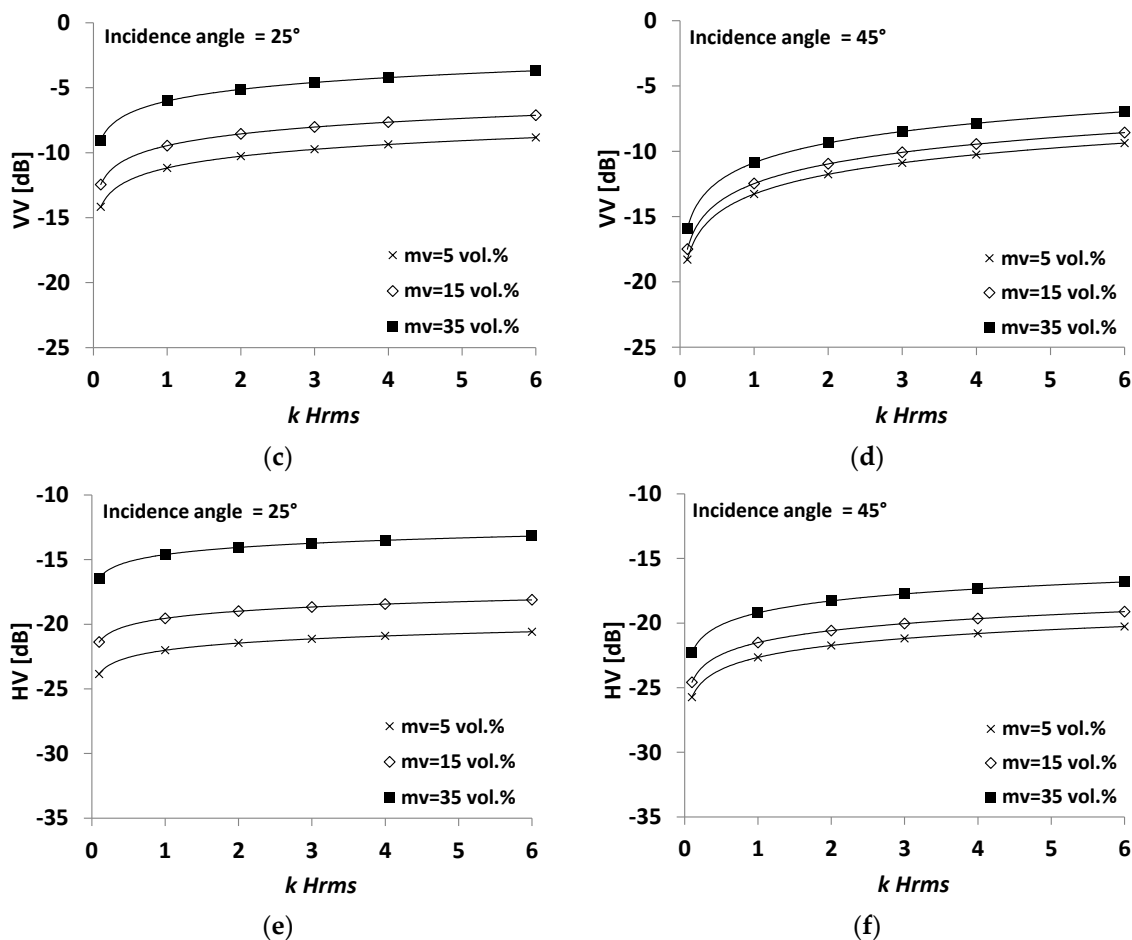

(a)　　　　　　　　　　　　　　　　　　(b)

Figure 6. *Cont.*

Figure 6. Behavior of the new model as a function of incidence angle (*θ*), surface roughness (*k Hrms*) and soil moisture (*mv*) in HH (**a** and **b**), VV (**c** and **d**), and HV (**e** and **f**) polarizations. (**a**,**c**,**e**): *θ* = 25°; (**b**,**d**,**f**): *θ* = 45°.

As mentioned in Dubois et al. [12], the ratio $\frac{\sigma^{\circ}_{HH}}{\sigma^{\circ}_{VV}}$ should increase with *kHrms* and remain less than 1. The new model shows that this condition is satisfied when $20° < θ < 45°$, *kHrms* < 6 and *mv* < 35 vol%.

5. Conclusions

This investigation's objective is to propose a new empirical model for radar backscatter from bare soil surfaces. The new model is based on the formulation made in the Dubois model where the radar signal in HH and VV polarizations is described according to radar wavelength, incidence angle, soil moisture, and roughness. This new model is based on the formulation made in the Dubois model. A large dataset was used, composed of ground measurements and SAR images over bare agricultural soils.

Results show that the new model provides improved results in comparison to the Dubois model (in the case of HH and VV). Biases and RMSE have decreased for both HH and VV polarizations. In addition, the high over- or under-estimations observed with the Dubois model for some ranges of soil moisture, surface roughness, and radar incidence angles were clearly eliminated with the new model. Analysis of the new model's performance for each radar wavelength separately (L, C, and X) shows that, in the L-band, the performance of the new model was similar to that of the Dubois model. The model shows significant improvement in C- and X-bands (RMSE approximately 1.9 dB with the new model and between 2.6–4.1 dB with the Dubois model).

Based on the same equation as that used for HH and VV, a radar signal in HV polarization was also proposed. Finally, the new empirical model proposed in the present study would allow more accurate soil moisture estimates using the new Sentinel-1A and -1B SAR data.

Author Contributions: Nicolas Baghdadi conceived the study; Nicolas Baghdadi performed the modeling Nicolas Baghdadi, Mohammad Choker and Mohammad El Hajj analyzed the results; Nicolas Baghdadi wrote the paper; Nicolas Baghdadi, Mohammad Choker, Mehrez Zribi, Mohammad El Hajj, Simonetta Paloscia, Niko E. C. Verhoest, Hans Lievens, Frederic Baup and Francesco Mattia revised the paper.

Conflicts of Interest: The authors declare no conflict of interest.

References

1. Rao, S.S.; Kumar, S.D.; Das, S.N. Modified Dubois model for estimating soil moisture with dual polarized SAR data. *J. Indian Soc. Remote Sens.* **2013**, *41*, 865–872.

2. Chai, X.; Zhang, T.T.; Shao, Y.; Gong, H.Z.; Liu, L.; Xie, K.X. Modeling and mapping soil moisture of plateau pasture using RADARSAT-2 imagery. *Remote Sens.* **2015**, *7*, 1279–1299.

3. Kirimi, F.; Kuria, D.N.; Frank Thonfeld, F.; Amler, E.; Mubea, K.; Misana, S.; Gunter Menz, G. Influence of vegetation cover on the Oh soil moisture retrieval model: A case study of the Malinda Wetland, Tanzania. *Adv. Remote Sens.* **2016**, *5*, 28–42.

4. Gherboudj, I.; Magagi, R.; Berg, A.A.; Toth, B. Soil moisture retrieval over agricultural Felds from multi-polarized and multi-angular RADARSAT-2 SAR data. *Remote Sens. Environ.* **2011**, *115*, 33–43. [CrossRef]

5. Zribi, M.; Chahbi, A.; Shabou, M.; Lili-Chabaane, Z.; Duchemin, B.; Baghdadi, N.; Amri, R.; Chehbouni, A. Soil surface moisture estimation over a semi-arid region using ENVISAT ASAR radar data for soil evaporation evaluation. *Hydrol. Earth Syst. Sci.* **2011**, *15*, 345–358. [CrossRef]

6. Le Hegarat-Mascle, S.; Zribi, M.; Alem, F.; Weisse, A.; Loumagne, C. Soil moisture estimation from ERS/SAR data: Toward an operational methodology. *IEEE Trans. Geosci. Remote Sens.* **2002**, *40*, 2647–2658. [CrossRef]

7. Zribi, M.; Dechambre, M. A new empirical model to retrieve soil moisture and roughness from Radar Data. *Remote Sens. Environ.* **2003**, *84*, 42–52. [CrossRef]

8. Oh, Y.; Sarabandi, K.; Ulaby, F.T. An empirical model and an inversion technique for radar scattering from bare soil surfaces. *IEEE Trans. Geosci. Remote Sens.* **1992**, *30*, 370–381. [CrossRef]

9. Oh, Y.; Kay, Y. Condition for precise measurement of soil surface roughness. *IEEE Trans. Geosci. Remote Sens.* **1998**, *36*, 691–695.

10. Oh, Y.; Sarabandi, K.; Ulaby, F.T. Semi-empirical model of the ensemble-averaged differential Mueller matrix for microwave backscattering from bare soil surfaces. *IEEE Trans. Geosci. Remote Sens.* **2002**, *40*, 1348–1355. [CrossRef]

11. Oh, Y. Quantitative retrieval of soil moisture content and surface roughness from multipolarized radar observations of bare soil surfaces. *IEEE Trans. Geosci. Remote Sens.* **2004**, *42*, 596–601. [CrossRef]

12. Dubois, P.C.; Van Zyl, J.; Engman, T. Measuring soil moisture with imaging radars. *IEEE Trans. Geosci. Remote Sens.* **1995**, *33*, 915–926. [CrossRef]

13. Baghdadi, N.; Saba, E.; Aubert, M.; Zribi, M.; Baup, F. Comparison between backscattered TerraSAR signals and simulations from the radar backscattering models IEM, Oh, and Dubois. *IEEE Geosci. Remote Sens. Lett.* **2011**, *8*, 1160–1164. [CrossRef]

14. Baghdadi, N.; Zribi, M. Evaluation of radar backscatter models IEM, Oh and Dubois using experimental observations. *Int. J. Remote Sens.* **2006**, *27*, 3831–3852. [CrossRef]

15. Wang, H.; Méric, S.; Allain, S.; Pottier, E. Adaptation of Oh Model for soil parameters retrieval using multi-angular RADARSAT-2 datasets. *J. Surv. Mapp. Eng.* **2014**, *2*, 65–74.

16.　Wang, J.R.; Hsu, A.; Shi, J.C.; O'Neill, P.E.; Engman, E.T. A comparison of soil moisture retrieval models using SIR-C measurements over the Little Washita River watershed. *Remote Sens. Environ.* **1997**, *59*, 308–320. [CrossRef]

17.　Zribi, M.; Taconet, O.; Le Hégarat-Mascle, S.; Vidal-Madjar, D.; Emblanch, C.; Loumagne, C.; Normand, M. Backscattering behavior and simulation comparison over bare soils using SIRC/XSAR and ERASME 1994 data over Orgeval. *Remote Sens. Environ.* **1997**, *59*, 256–266. [CrossRef]

18.　Baghdadi, N.; Dubois-Fernandez, P.; Dupuis, X.; Zribi, M. Sensitivity of mail polarimetric parameters of multifrequency polarimetric SAR data to soil moisture and surface roughness over bare agricultural soils. *IEEE Geosci. Remote Sens. Lett.* **2013**, *10*, 731–735. [CrossRef]

19.　Baghdadi, N.; Zribi, M.; Loumagne, C.; Ansart, P.; Paris Anguela, T. Analysis of TerraSAR-X data and their sensitivity to soil surface parameters over bare agricultural fields. *Remote Sens. Environ.* **2008**, *112*, 4370–4379. [CrossRef]

20.　Baghdadi, N.; Aubert, M.; Zribi, M. Use of TerraSAR-X data to retrieve soil moisture over bare soil agricultural fields. *IEEE Geosci. Remote Sens. Lett.* **2012**, *9*, 512–516. [CrossRef]

21.　Baghdadi, N.; Gherboudj, I.; Zribi, M.; Sahebi, M.; Bonn, F.; King, C. Semi-empirical calibration of the IEM backscattering model using radar images and moisture and roughness field measurements. *Int. J. Remote Sens.* **2004**, *25*, 3593–3623. [CrossRef]

22.　Baghdadi, N.; King, C.; Bourguignon, A.; Remond, A. Potential of ERS and RADARSAT data for surface roughness monitoring over bare agricultural fields: Application to catchments in Northern France. *Int. J. Remote Sens.* **2002**, *23*, 3427–3442. [CrossRef]

23.　Holah, H.; Baghdadi, N.; Zribi, M.; Bruand, A.; King, C. Potential of ASAR/ENVISAT for the characterisation of soil surface parameters over bare agricultural fields. *Remote Sens. Environ.* **2005**, *96*, 78–86. [CrossRef]

24.　Baghdadi, N.; Holah, N.; Zribi, M. Calibration of the Integral Equation Model for SAR data in C-band and HH and VV polarizations. *Int. J. Remote Sens.* **2006**, *27*, 805–816. [CrossRef]

25.　Le Morvan, A.; Zribi, M.; Baghdadi, N.; Chanzy, A. Soil moisture profile effect on radar signal measurement. *Remote Sens.* **2008**, *8*, 256–270. [CrossRef]

26.　Baghdadi, N.; Cresson, R.; El Hajj, M.; Ludwig, R.; La Jeunesse, I. Estimation of soil parameters over bare agriculture areas from C-band polarimetric SAR data using neural networks. *Hydrol. Earth Syst. Sci. (HESS)* **2012**, *16*, 1607–1621. [CrossRef]

27.　Baghdadi, N.; Aubert, M.; Cerdan, O.; Franchistéguy, L.; Viel, C.; Martin, E.; Zribi, M.; Desprats, J.F. Operational mapping of soil moisture using synthetic aperture radar data: Application to Touch basin (France). *Sens. J.* **2007**, *7*, 2458–2483. [CrossRef]

28.　Zribi, M.; Gorrab, A.; Baghdadi, N.; Lili-Chabaane, Z. Influence of radar frequency on the relationship between bare surface soil moisture vertical profile and radar backscatter. *IEEE Geosci. Remote Sens. Lett.* **2014**, *11*, 848–852. [CrossRef]

29.　Gorrab, A.; Zribi, M.; Baghdadi, N.; Mougenot, B.; Lili-Chabaane, Z. Retrieval of both soil moisture and texture using TerraSAR-X images. *Remote Sens.* **2015**, *7*, 10098–10116. [CrossRef]

30.　Aubert, M.; Baghdadi, N.; Zribi, M.; Ose, K.; El Hajj, M.; Vaudour, E.; Gonzalez-Sosa, E. Toward an operational bare soil moisture mapping using TerraSAR-X data acquired over agricultural areas. *IEEE J. Sel. Top. Appl. Earth Obs. Remote Sens. (JSTARS)* **2013**, *6*, 900–916. [CrossRef]

31.　Dong, L.; Baghdadi, N.; Ludwig, R. Retrieving surface soil moisture using radar imagery in a semi-arid environment. *IEEE Geosci. Remote Sens. Lett.* **2013**, *10*, 461–465. [CrossRef]

32.　Baup, F.; Fieuzal, R.; Marais-Sicre, C.; Dejoux, J.-F.; le Dantec, V.; Mordelet, P.; Claverie, M.; Hagolle, O.; Lopes, A.; Keravec, P.; et al. MCM'10: An experiment for satellite multi-sensors crop monitoring. In *From High to Low Resolution Observations, IEEE International Geoscience and Remote Sensing Symposium*, Munich, Germany, 22–27 July 2012.

33.　Mattia, M.; Toan, T.L.; Souyris, J.C.; Carolis, G.D.; Floury, N.; Posa, F.; Pasquariello, G. The effect of surface roughness on multifrequency polarimetric SAR data. *IEEE Trans. Geosci. Remote Sens.* **1997**, *35*, 954–966. [CrossRef]

34.　Lievens, H.; Verhoest, N.E.C.; De Keyser, E.; Vernieuwe, H.; Matgen, P.; Álvarez-Mozos, J.; De Baets, B. Effective roughness modelling as a tool for soil moisture retrieval from C-and L-band SAR. *Hydrol. Earth Syst. Sci.* **2011**, *15*, 151–162. [CrossRef]

35. Baronti, S.; Del Frate, F.; Ferrazzoli, P.; Paloscia, S.; Pampaloni, P.; Schiavon, G. SAR polarimetric features of agricultural areas. *Int. J. Remote Sens.* **1995**, *16*, 2639–2656. [CrossRef]

36. Macelloni, G.; Paloscia, S.; Pampaloni, P.; Sigismondi, S.; de Matthæis, P.; Ferrazzoli, P.; Schiavon, G.; Solimini, D. The SIR-C/X-SAR experiment on Montespertoli: Sensitivity to hydrological parameters. *Int. J. Remote Sens.* **1999**, *20*, 2597–2612. [CrossRef]

37. Paloscia, S.; Macelloni, G.; Pampaloni, P.; Sigismondi, S. The potential of C- and L-band SAR in estimating vegetation biomass: The ERS-1 and JERS-1 Experiments. *IEEE Trans. Geosci. Remote Sens.* **1999**, *37*, 2107–2110. [CrossRef]

38. Ulaby, F.T.; Moore, R.K.; Fung, A.K. *Microwave Remote Sensing*; Addison-Wesley: New York, NY, USA, 1982.

39. Beauchemin, M.; Thomson, K.; Edwards, G. Modelling forest stands with MIMICS: Implications for calibration. *Can. J. Remote Sens.* **1995**, *21*, 518–526. [CrossRef]

40. Baghdadi, N.; Bernier, M.; Gauthier, R.; Neeson, I. Evaluation of C-band SAR data for wetlands mapping. *Int. J. Remote Sens.* **2001**, *22*, 71–88. [CrossRef]

41. Baghdadi, N.; Holah, N.; Zribi, M. Soil moisture estimation using multi-incidence and multi-polarization ASAR SAR data. *Int. J. Remote Sens.* **2006**, *27*, 1907–1920. [CrossRef]

42. Aubert, M.; Baghdadi, N.; Zribi, M.; Douaoui, A.; Loumagne, C.; Baup, F.; El Hajj, M.; Garrigues, S. Characterization of soil surface by TerraSAR-X imagery. *Remote Sens. Environ.* **2011**, *115*, 1801–1810. [CrossRef]

43. Baghdadi, N.; Cerdan, O.; Zribi, M.; Auzet, V.; Darboux, F.; El Hajj, M.; Bou Kheir, R. Operational performance of current synthetic aperture radar sensors in mapping soil surface characteristics in agricultural environments: Application to hydrological and erosion modelling. *Hydrol. Process.* **2008**, *22*, 9–20. [CrossRef]

44. Srivastava, H.S.; Patel, P.; Manchanda, M.L.; Adiga, S. Use of multi-incidence angle RADARSAT-1 SAR data to incorporate the effects of surface roughness in soil moisture estimation. *IEEE Trans. Geosci. Remote Sens.* **2003**, *41*, 1638–1640. [CrossRef]

45. Sahebi, M.R.; Angles, J.; Bonn, F. A comparison of multi-polarization and multi-angular approaches for estimating bare soil surface roughness from spaceborne radar data. *Can. J. Remote Sens.* **2002**, *28*, 641–652. [CrossRef]

46. Fung, A.K. *Microwave Scattering and Emission Models and Their Applications*; Artech House, Inc.: Boston, MA, USA, 1994.